

Mixed-Mode Crack Propagation in Functionally Graded Materials

Jeong-Ho Kim^{1,a} and Glaucio H. Paulino^{2,b}

¹Department of Civil and Environmental Engineering, University of Connecticut, Storrs, CT 06269, USA

²Department of Civil and Environmental Engineering University of Illinois, Urbana, IL 61801, USA
^ajhkim@engr.uconn.edu, ^bpaulino@uiuc.edu

Keywords: Functionally graded materials. Finite element method. Interaction integral method. Crack propagation.

Abstract. This paper presents numerical simulation of mixed-mode crack propagation in functionally graded materials by means of a remeshing algorithm in conjunction with the finite element method. Each step of crack growth simulation consists of the calculation of the mixed-mode stress intensity factors by means of a non-equilibrium formulation of the interaction integral method, determination of the crack growth direction based on a specific fracture criterion, and local automatic remeshing along the crack path. A specific fracture criterion is tailored for FGMs based on the assumption of local homogenization of asymptotic crack-tip fields in FGMs. The present approach uses a user-defined crack increment at the beginning of the simulation. Crack trajectories obtained by the present numerical simulation are compared with available experimental results.

Introduction

Functionally graded materials (FGMs) are multifunctional composites involving spatially varying volume fractions of constituent materials, thus providing a graded microstructure and macroproperties [1,2,3]. These materials have been introduced to take advantage of ideal behavior of material constituents. For instance, partially stabilized zirconia (PSZ) shows high resistance to heat and corrosion, and CrNi alloy has high mechanical strength and toughness (see Fig. 1) [4]. FGMs have been used in many engineering applications [1,2,3] including graded cathodes in solid oxide fuel cells (SOFCs) [5]. Due to multifunctional capabilities, FGMs have been investigated for various damage and failure mechanisms under mechanical or thermal loads, and static, dynamic or fatigue loads, etc [2,3].

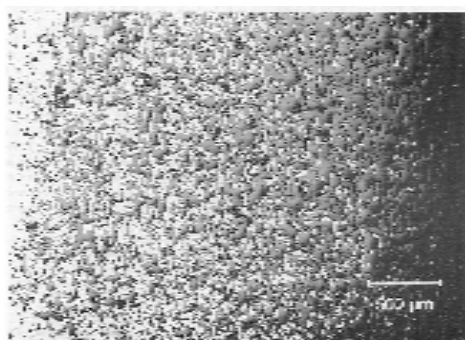


Fig. 1: Micrograph illustrating graded transition region between CrNi alloy and partially stabilized zirconia (PSZ) [4].

Crack Growth Simulation

Crack growth simulation is performed by means of the I-FRANC2D (Illinois-FRANC2D) code [6], which is based on FRANC2D (FRacture Analysis Code 2D) [7]. The I-FRANC2D is capable of evaluating mixed-mode stress intensity factors (SIFs) for FGMs which are used to determine crack initiation angles (θ_0). Finite element-based crack growth simulation involves a series of steps. Fig. 2 illustrates crack propagation procedure at each step [6,7].

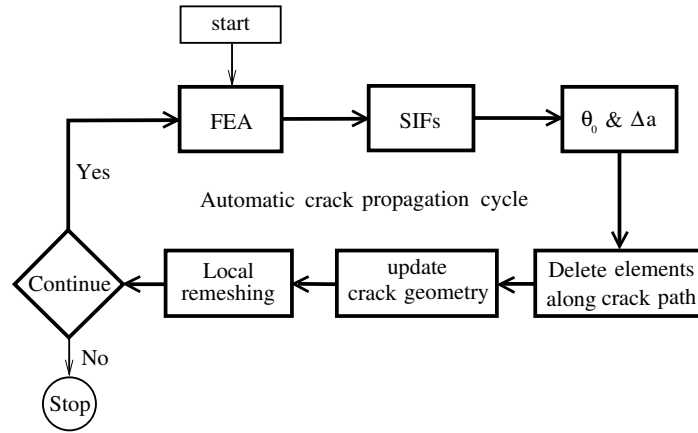


Fig. 2: Automatic crack propagation procedure used in the I-FRANC2D code.

At each crack propagation cycle, crack initiation condition must be assessed for determining whether the crack will grow or not. Fig. 3 shows a fracture locus involving mode I and II SIFs and fracture toughness K_{Ic} . If the crack driving force is big enough for the crack-tip fields to reach the fracture envelope, then the crack does grow.

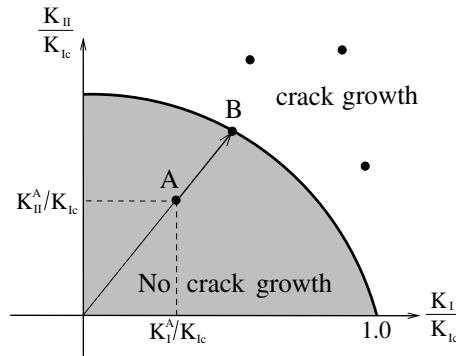


Fig. 3: Fracture locus involving mode I and II SIFs and fracture toughness.

The Interaction Integral Method

The interaction integral (M-integral) method is an accurate scheme to evaluate SIFs in FGMs [8,9]. Here we adopt a non-equilibrium formulation [6,10], which uses displacement and strain fields developed for homogeneous materials, and employ the non-equilibrium stress fields $\sigma^{aux} = C(x) \epsilon^{aux}$, where $C(x)$ is the FGM stiffness tensor, σ^{aux} is the auxiliary stress, and ϵ^{aux} is the auxiliary strain. The interaction integral is derived from the path-independent J -integral [11] for two admissible states (actual and auxiliary) of a cracked elastic FGM body. The so-called M -integral, based on the non-equilibrium formulation, is obtained as [6,10]

$$M = \int_A (\sigma_{ij} u_{i,1}^{aux} + \sigma_{ij}^{aux} u_{i,1} - \sigma_{ik} \epsilon_{ik}^{aux} \delta_{1j}) q_{,j} dA + \int_A (\underline{\sigma_{ij,j}^{aux} u_{i,1}} - C_{ijkl} \epsilon_{kl} \epsilon_{ij}^{aux}) q dA, \quad (1)$$

where u_i , ϵ_{ij} and σ_{ij} are the actual displacement, strain and stress fields, respectively; q is a weight function which varies from 1 on the inner contour to 0 on the outer contour; and the underlined term is a non-equilibrium term, which appears due to non-equilibrium of the auxiliary stress fields. The relationship between M -integral and SIFs (K_I, K_{II}) is given by

$$M = 2(K_I K_I^{aux} + K_{II} K_{II}^{aux}) / E_{tip}^*, \quad (2)$$

where $E_{tip}^* = E_{tip}$ for plane stress and $E_{tip}^* = E_{tip} / (1 - \nu^2)$ for plane strain. The mode I and mode II SIFs are evaluated as follows:

$$\begin{aligned} K_I &= M^{(1)} E_{tip}^* / 2, \quad (K_I^{aux} = 1.0, K_{II}^{aux} = 0.0) \\ K_{II} &= M^{(2)} E_{tip}^* / 2, \quad (K_I^{aux} = 0.0, K_{II}^{aux} = 1.0) \end{aligned} \quad (3)$$

The above SIF relationships of Eq. 3 are the same as those for homogeneous materials [12] except that, for FGMs, the material properties are evaluated at the crack-tip location [13].

A Fracture Criterion for FGMs

The singularity and angular functions of asymptotic crack-tip fields for FGMs are the same as for homogeneous materials [13]. Thus local homogenization arguments may allow the use of fracture criteria originally developed for homogeneous materials. Here we adopt the maximum energy release rate criterion proposed by Hussain *et al.* [14]. The energy release rate is given by [14]

$$G(\theta) = \frac{4}{E_{tip}^*} \left(\frac{1}{3 + \cos^2 \theta} \right)^2 \left(\frac{1 - \pi/\theta}{1 + \pi/\theta} \right)^{0/\pi} \left[(1 + 3\cos^2 \theta) K_I^2 + 8\sin \theta \cos \theta K_I K_{II} + (9 - 5\cos^2 \theta) K_{II}^2 \right]. \quad (4)$$

Then the crack initiation angle θ_0 is obtained from [14]

$$\partial G(\theta) / \partial \theta = 0, \quad \partial^2 G(\theta) / \partial \theta^2 < 0 \Rightarrow \theta = \theta_0. \quad (5)$$

The crack initiation condition is given by

$$G(\theta_0) = G_c(x), \quad (6)$$

where $G_c(x)$ is the critical energy release rate function. Ideally, the function $G_c(x)$ should be obtained from experiments.

Crack Growth in an Epoxy/Glass FGM Beam

Rousseau and Tippur [15] investigated crack growth behavior of a crack normal to the material gradient in an epoxy/glass (50 vol%) FGM beam subjected to four-point bending. Fig. 4 shows specimen geometry and boundary conditions (BCs) of the FGM beam with a crack located at $\xi=0.37$. Table 1 shows the numerical values of material properties at interior points in the graded region. Material properties in the intermediate regions vary linearly.

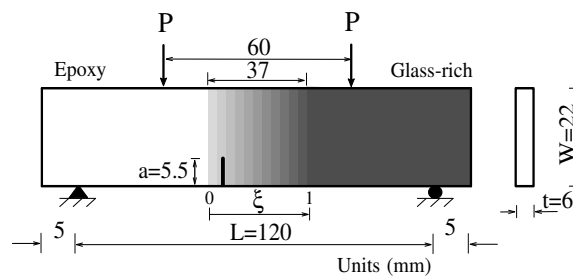


Fig. 4: Geometry and BCs of the epoxy/glass FGM beam

Table 1: Material properties (Young's modulus (E), Poisson's ratio (ν) and fracture toughness (K_{Ic})) at interior points in the graded region (defined by the parameter ξ).

ξ	$E(\text{MPa})$	ν	$K_{Ic} (\text{MPam}^{1/2})$
0.00	3000	0.35	1.2
0.17	3300	0.34	2.1
0.33	5300	0.33	2.7
0.58	7300	0.31	2.7
0.83	8300	0.30	2.6
1.00	8600	0.29	2.6

The following data are used for the FEM analyses: plane stress, $a/W=0.25$, $t=6$, $P=P_{cr}(a+n\Delta a, X)$, where n refers to the number of crack propagation increments, Δa denotes a crack increment, and $X=(X_1, X_2)$ denotes crack locations. Fig. 5(a) compares experimental results for crack trajectory with those of numerical simulation ($\Delta a=1\text{mm}$). There is good agreement between two results. Moreover, experimental and numerical results for the crack initiation angle at the initial step are in good agreement, i.e. $\theta_{\text{exp}}=7^\circ$ and $\theta_{\text{num}}=6.98^\circ$, respectively. Figs. 5(b) and 5(c) show finite element discretizations at the initial and final steps, respectively, of crack propagation considering $\Delta a=1\text{mm}$.

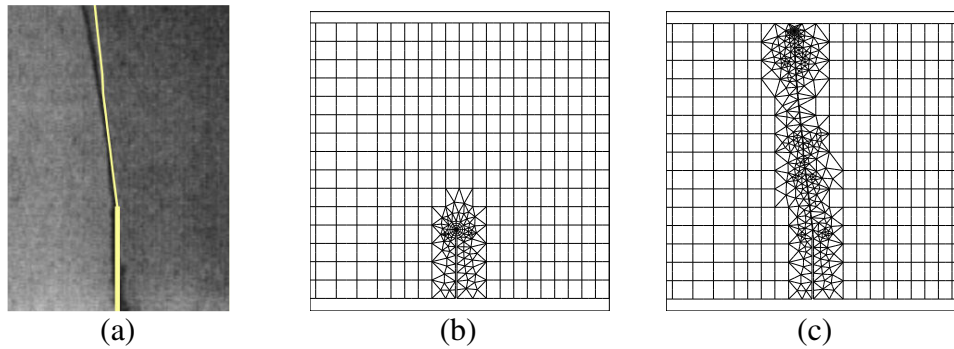


Fig. 5: Experimental and numerical results: (a) Comparison of crack trajectory in the region $0 \leq W \leq 16.5\text{mm}$; finite element discretizations at the (b) initial (step 0) and (c) final step (step 16) of crack propagation.

Here we calculated the critical load at each step based on the maximum energy release rate and applied the calculated critical load to the corresponding step of crack propagation. Table 2 shows numerical results at the initial step for the critical load P_{cr} , SIFs (K_I, K_{II}), phase angle $\psi = \tan^{-1}(K_{II}/K_I)$, and the crack initiation angle θ_o . Because $K_{II} < 0$, the crack initiation angle θ_o is counter-clockwise with respect to the crack line (see Fig. 5(a)).

Table 2: Numerical results for the critical load P_{cr} , Mode I and II SIFs, phase angle $\psi = \tan^{-1}(K_{II}/K_I)$, and the crack initiation angle θ_o at the initial step.

$P_{cr} (\text{N})$	$K_I (\text{MPam}^{1/2})$	$K_{II} (\text{MPam}^{1/2})$	ψ	θ_o
253.5	2.122	-0.129	-3.484	6.98°

Conclusions

This paper presents automatic simulation of crack propagation in FGMs by means of a remeshing scheme in conjunction with the finite element method. Based on local homogenization, we use the maximum energy release rate criterion. Crack trajectories obtained by this fracture criterion agree well with available experimental results for FGMs. The computational scheme developed here serves as a guideline for fracture experiments on FGM specimens (e.g. initiation toughness and R-curve behavior).

Acknowledgement

We gratefully acknowledge the support from the NASA Ames Research Center, NAG 2-1424 (Chief Engineer, Dr. Tina Panontin), and the National Science Foundation (NSF) under grant CMS-0115954 (Mechanics and Materials Program).

References

- [1] T. Hirai. *Proceedings of the Second International Symposium on Functionally Graded Materials*, volume 34 of *Ceramic Transactions* (J.B. Holt, M. Koizumi, T. Hirai and Z.A. Munir, editors, The American Ceramic Society, Westerville, Ohio, 1993), p. 11.
- [2] S. Suresh and A.Q. Mortensen: *Fundamentals of Functionally Graded Materials* (IOM Communications Ltd, London, 1998).
- [3] G.H. Paulino, Z.H. Jin and R.H. Dodds Jr: *Comprehensive Structural Integrity* (B. Karihaloo and W.G. Knauss, editors, volume 2, Chapter 13, Elsevier Science, 2003), p. 607.
- [4] B. Ilshner: *Journal of the Mechanics and Physics of Solids* Vol. 44(5), p. 647.
- [5] N.T. Hart, N.P. Brandon, M.J. Day and J.E. Shemilt: *Journal of Materials Science* Vol. 36 (2001), p. 1077.
- [6] J.H. Kim: *Mixed-mode crack propagation in functionally graded materials*, Ph.D. Thesis, University of Illinois at Urbana-Champaign, Illinois, 2003.
- [7] P.A. Wawrzynek: *Interactive finite element analysis of fracture processes: An integrated approach*, M.S. Thesis, Cornell University, 1987.
- [8] J. Dolbow and M. Gosz: *International Journal of Solids and Structures* Vol. 39 (9) (2002), p. 2557.
- [9] J.H. Kim and G.H. Paulino: *Computer Methods in Applied Mechanics and Engineering* Vol. 192 (11-12) (2003), p. 1463.
- [10] G.H. Paulino and J.H. Kim: *Engineering Fracture Mechanics* Vol. 71 (13-14) (2004), p. 1907.
- [11] J.R. Rice: *ASME Journal of Applied Mechanics* Vol. 35 (2) (1968), p. 379.
- [12] J.F. Yau, S.S. Wang and H.T. Corten: *ASME Journal of Applied Mechanics* Vol. 47 (2) (1980), p.335.
- [13] J.W. Eischen: *International Journal of Fracture* Vol. 34 (1) (1987), p. 3.
- [14] M.A. Hussain, S.L. Pu and J. Underwood: *Fracture Analysis* (P.C. Paris and G.R. Irwin, editors, ASTM STP 560, American Society for Testing and Materials, Philadelphia, PA, 1993), p. 2.
- [15] C.E. Rousseau and H.V. Tippur: *Acta Materialia* Vol. 48 (16) (2000), p. 4021.

Functionally Graded Materials VIII

doi:10.4028/www.scientific.net/MSF.492-493

Mixed-Mode Crack Propagation in Functionally Graded Materials

doi:10.4028/www.scientific.net/MSF.492-493.409